Expression and Characterization of a Four-α-Helix Bundle Protein That Binds the Volatile General Anesthetic Halothane

Ravindernath Pidikiti,[†] Mohammad Shamim,[‡] Krishna M. G. Mallela,[§] Konda S. Reddy,[§] and Jonas S. Johansson*[,†,§,||]

Departments of Anesthesia, Internal Medicine, and Biochemistry and Biophysics, and the Johnson Research Foundation, University of Pennsylvania, Philadelphia, Pennsylvania 19104

Received December 6, 2004; Revised Manuscript Received January 20, 2005

The structural features of volatile anesthetic binding sites on proteins are being investigated with the use of a defined model system consisting of a four-α-helix bundle scaffold with a hydrophobic core. The current study describes the bacterial expression, purification, and initial characterization of the four-α-helix bundle $(A\alpha_2\text{-L1M/L38M})_2$. The α-helical content and stability of the expressed protein are comparable to that of the chemically synthesized four-α-helix bundle $(A\alpha_2\text{-L38M})_2$ reported earlier (Johansson, J. S.; Scharf, D.; Davies, L. A.; Reddy, K. S.; Eckenhoff, R. G. *Biophys. J.* **2000**, *78*, 982). The affinity for binding halothane is somewhat improved with a $K_d = 120 \pm 20\ \mu M$ as determined by W15 fluorescence quenching, attributed to the L1M substitution. Near-UV circular dichroism spectroscopy demonstrated that halothane binding changes the orientation of the aromatic residues in the four-α-helix bundle. Nuclear magnetic resonance experiments reveal that halothane binding results in narrowing of the peaks in the amide region of the one-dimensional proton spectrum, indicating that bound anesthetic limits protein dynamics. This expressed protein should prove to be amenable to nuclear magnetic resonance structural studies on the anesthetic complexes, because of its relatively small size (124 residues) and the high affinities for binding volatile anesthetics. Such studies will provide much needed insight into how volatile anesthetics interact with biological macromolecules and will provide guidelines regarding the general architecture of binding sites on central nervous system proteins.

Introduction

A molecular understanding of volatile general anesthetic mechanisms of action will require structural descriptions of anesthetic−protein complexes. Because the in vivo sites of action remain to be determined, the structural features of anesthetic binding sites on proteins are being explored using well-defined model systems, such as the serum albumins and four-α-helix bundle proteins.[2] Studies with these model systems suggest that volatile general anesthetics preferentially bind to preexisting appropriately sized packing defects, or cavities, within the protein matrix. The overall volume of the packing defect appears to modulate anesthetic binding affinity over approximately a 2-fold range.[3] In addition, favorable polar interactions with hydrophobic core side-chains can further enhance anesthetic binding affinity.[1,4]

Previous work using fluorescence quenching has demonstrated that the halogenated alkane volatile anesthetics halothane and chloroform bind to the designed packing defect in the hydrophobic core of the chemically synthesized four-α-helix bundle $(A\alpha_2\text{-L38M})_2$ with dissociation constants that are comparable to their clinical EC_{50} values.[1,5] Isothermal titration calorimetry revealed that the halogenated ether anesthetics isoflurane, enflurane, sevoflurane, and desflurane also bound to the hydrophobic core of the four-α-helix bundle $(A\alpha_2\text{-L38M})_2$ with dissociation constants that mirror their clinical EC_{50} values.[6,7] These studies indicate that the four-α-helix bundle $(A\alpha_2\text{-L38M})_2$ represents a reasonable model for the in vivo central nervous system sites of anesthetic action.

The currently favored targets for the volatile general anesthetics include the ligand-gated ion channels such as the γ-aminobutyric acid type A receptor and the glycine receptor.[8] Although the structures of these membrane proteins remain unclear, a recent electron cryomicroscopy study on the related nicotinic acetylcholine receptor from *Torpedo marmorata* at 4 Å resolution indicates that the transmembrane domain of each subunit consists of a four-α-helix bundle.[9] The expressed four-α-helix bundle (Figure 1) is therefore proposed to serve as a scaled-down model for the lipid-spanning domains of these and other membrane proteins. The rationale for this approach is supported by the evidence that the membrane-embedded domains of proteins such as the nicotinic acetylcholine receptor[10,11] and bovine rhodopsin[12] may interact directly with volatile general anesthetics.

In this manuscript, the successful cloning and expression of $(A\alpha_2\text{-L1M/L38M})_2$ in *Escherichia coli* is described, along with the characterization of the protein secondary structure and stability. Binding of the volatile general anesthetic halothane to the four-α-helix bundle protein is demonstrated

* To whom correspondence should be addressed. Telephone: 215-349-5472. Fax: 215-349-5078. E-mail: johanssj@uphs.upenn.edu.
[†] Department of Anesthesia.
[‡] Department of Internal Medicine.
[§] Department of Biochemistry and Biophysics.
[||] Johnson Research Foundation.

10.1021/bm049226a CCC: $30.25
Published on Web 02/25/2005

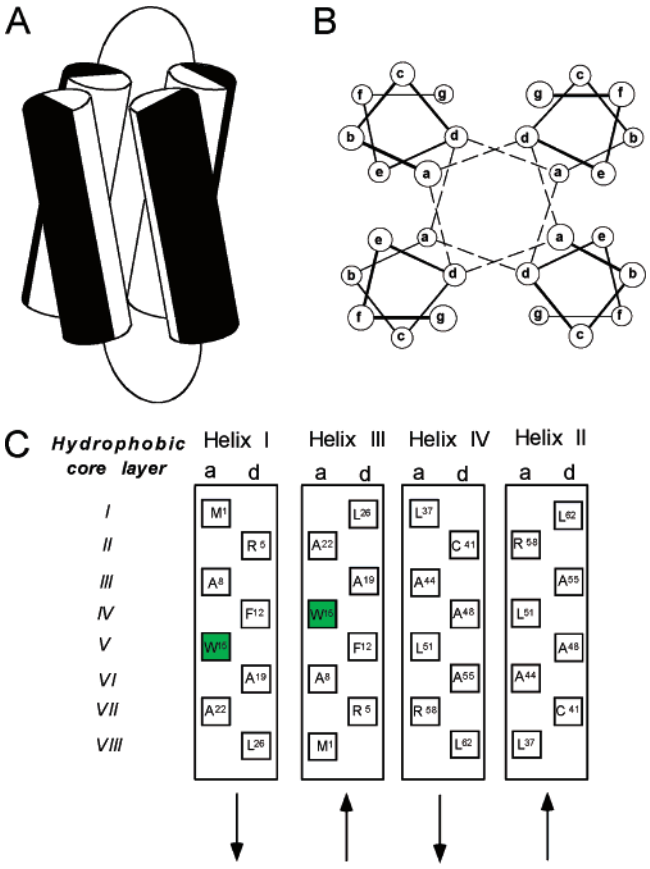

Figure 1. (A) Modeled structure of the expressed four-α-helix bundle $(A\alpha_2\text{-L1M/L38M})_2$. The cylinders represent the two 27-residue amphiphilic α-helical portions of each 62-residue di-α-helical peptide, joined by an eight-residue glycine linker. Black and white halves of each cylinder represent hydrophilic and hydrophobic residues, respectively. (B) End-on view of the anti four-α-helix bundle, showing the interaction of the hydrophobic core residues at the heptad a and d positions. The dashed lines indicate how successive hydrophobic core layers are composed of two a and two d residues. (C) An opened-out and flattened representation of the $(A\alpha_2\text{-L1M/L38M})_2$ bundle illustrating the residues present at the hydrophobic heptad a and d positions. There are a total of eight hydrophobic core layers, each composed of two a and two d position residues. The heptad a W15 residues are shaded. Equivalent binding sites for anesthetic molecules reside in hydrophobic core layers III and VI where larger leucines were replaced with smaller alanines.[15]

using tryptophan fluorescence quenching.[13] Far-UV circular dichroism spectroscopy and nuclear magnetic resonance spectroscopy reveal that halothane binding is associated with structural changes in the protein. The ability to express this four-α-helix bundle protein in a bacterial system sets the stage for future high-resolution nuclear magnetic resonance structural studies on the protein in the presence of bound anesthetic molecules.

Materials and Methods

Materials. Halothane (2-bromo-2-chloro-1,1,1-trifluoroethane) was obtained from Halocarbon Laboratories (Hackensack, NJ). The thymol preservative present in the commercial halothane was removed with an aluminum oxide column.[13] Oligonucleotides were purchased from Integrated DNA Technologies Inc. (Coralville, IA). These were synthesized on a 100 nmol scale, and stock solutions were

Met-Lys-Lys-Leu-Arg-Glu-Glu-Ala-Ala-Lys-Leu-Phe-Glu-Glu-Trp-Lys-Lys-Leu-Ala-Glu-Glu-Ala-Ala-Lys-Leu-Leu-Glu-Gly-Gly-Gly-Gly-Gly-Gly-Gly-Gly-Glu-Leu-Met-Lys-Leu-Cys-Glu-Glu-Ala-Ala-Lys-Lys-Ala-Glu-Glu-Leu-Phe-Lys-Leu-Ala-Glu-Glu-Arg-Leu-Lys-Lys-Leu

Figure 2. Primary structure of the expressed $A\alpha_2$-L1M/L38M protein.

prepared at a concentration of 200 μM in water without additional purification. All restriction enzymes, PCR kit components, and the plasmid cloning vector (pET-11a) were obtained from New England Biolabs (Beverly, MA). Competent *Escherichia coli* cells (DH5α and BL-21 (DE3) codon plus for protein expression) were purchased from Invitrogen Inc. (Carlsbad, CA). The QIA quick gel extraction kit and the QIA spin mini-prep kit were obtained from Qiagen Inc. (Valencia, CA), and isopropyl-D-thiogalactopyranoside (IPTG) was from Sigma Chemical Co. (St Louis, MO). All other chemicals were of reagent grade.

Design and Assembly of a Gene for the Helix-Loop-Helix Protein $A\alpha_2$-L1M/L38M. The coding and noncoding strand sequences were used to implement PCR-based assembly and amplification of a codon-optimized full length gene (189 bp) for the helix-loop-helix protein $A\alpha_2$-L1M/L38M (Figure 2) using a previously described protocol.[14] The $A\alpha_2$-L1M/L38M protein synthetic gene was designed using codons favored by *E. coli* class II genes (those that are expressed at high levels during exponential growth) for cloning and protein expression purposes. To facilitate cloning in the pET-11a plasmid vector, short artificial sequences were added to each end of the codon-optimized gene to provide an *Nde*I restriction site at the start codon, and a *Bam*HI restriction site downstream of the stop codon.

As shown in Figure 3, the first sense strand primer (S-1) is a 30-mer and consists of 18 nucleotides coding for the desired sequence at the 3′-terminal along with a 12 nucleotide flanking region at the 5′-terminal. Next, the 5′-terminal end of the first 15 nucleotide antisense strand primer (AS-1) is chosen to obtain the required number of overlapping base pairs with the 3′-terminal of the S-1 primer followed by a second antisense strand primer (AS-2) with 15 nucleotides of the 5′-terminal. The 5′-terminal end of the second 30 nucleotide sense strand primer (S-2) is then chosen to obtain the required number of overlapping base pairs with the 3′-terminal end of the second antisense strand primer (AS-2), and so on. Finally, the antisense strand primer (AS-8) is a 15 nucleotide sequence which fills in the overhang of the 3′-terminal of the last sense strand primer (S-7). This process is repeated until a complete set of sense- and antisense strand primers are generated for the entire DNA sequence.

The designed primer set (Figure 3) was used for gene assembly. Briefly, equal volumes of each of the 15 oligonucleotide solutions were combined and the mixture was subsequently diluted 100-fold in 20 μL of PCR mix containing 10 mM Tris-HCl at pH 9.0, 2.2 mM $MgCl_2$, 50 mM KCl, 0.2 mM of each dNTP/0.1% Triton-X-100, and 1 μL of the *Taq* DNA polymerase enzyme. The PCR program consisted of 55 cycles at 94 °C for 30 s, 52 °C for 30 s, and

SENSE-STRAND PRIMERS

S-1 5'-GGA GAT ATA CAT ATG CTG AAA AAA CTG CGT-3'
S-2 5'-GAA GAA GCG GCG AAA CTG TTC GAA GAA TGG-3'
S-3 5'-AAG AAA TTA GCA GAG GAG GCG GCT AAA TTA-3'
S-4 5'-TTG GAA GGC GGT GGT GGT GGC GGC GCT GAA-3'
S-5 5'-CTG ATG AAA TTA TGC GAG GAG GCA GCT AAA-3'
S-6 5'-AAG GCA GAA GAG CTG TTC AAA CTG GCA GAA-3'
S-7 5'-GAA CGT CTG AAG AAA CTG TAA GGA TCC GGC-3'

ANTISENSE-STRAND PRIMERS

AS-1 5'-CCT CTA TAT GTA TAC-3'
AS-2 5'-GAC TTT TTT GAC GCA CTT CTT CGC CGC TTT-3'
AS-3 5'-GAC AAG CTT CTT ACC TTC TTT AAT CGT CTC-3'
AS-4 5'-CTC CGC CGA TTT AAT AAC CTT CCG CCA CCA-3'
AS-5 5'-CCA CCG CCG CCT CTT GAC TAC TTT AAT ACG-3'
AS-6 5'-CTC CTC CGT CGA TTT TTC CGT CTT CTC GAC-3'
AS-7 5'-AAG TTT GAC CGT CTT CTT GCA GAC TTC TTT-3'
AS-8 5'-GAC ATT CCT AGG CCG-3'

Figure 3. Nucleotide sequences of the 15 primers used to construct the $A\alpha_2$-L1M/L38M gene.

72 °C for 30 s, in a Biometra T-gradient thermoblock (Biomedizinische Analytik GmbH, Göttingen, Germany).

The above gene assembly reaction mixture (2.5 μL) was diluted 40-fold in 100 μL of PCR mix as above with 5 μL of *Taq* DNA polymerase and with the outermost 5′-terminal sense strand primer (S-1) and the 5′-terminal antisense strand primer (AS-8) used at a concentration of 1 μM. The PCR program consisted of 23 cycles at 94 °C for 30 s, 50 °C for 30 s, and 72 °C for 60 s. The resulting DNA fragment corresponding to the length calculated for the given set of primers was verified using 2% agarose gel electrophoresis.

The full-length sequence of the $A\alpha_2$-L1M/L38M protein gene amplified DNA was obtained by two rounds of PCR as above. The resulting PCR product was purified and digested by *Nde*I and *Bam*HI, and ligated into the pET-11a plasmid vector with T_4 DNA ligase. The cloned pET-11a vector was transformed into the DH5α *E. coli* strain for sequencing and transformed into BL21 (DE3) codon plus *E. coli* cells for protein expression. The transformants were selected on ampicillin resistant agar plates. DNA sequencing (Cell Center, University of Pennsylvania, Philadelphia, PA) confirmed the identity of the gene.

Expression and Purification of $A\alpha_2$-L1M/L38M. Plasmid containing the $A\alpha_2$-L1M/L38M gene was transformed into BL21 (DE3) codon plus *E. coli* cells, and grown to log phase ($OD_{600nm} = 0.6-0.8$) in 1 L batches in LB medium at 37 °C. The growth medium was supplemented with 50 μg/mL ampicillin. Expression was induced by the addition of IPTG to a final concentration of 0.5 mM after the culture reached an $OD_{600} = 0.6-0.8$. The bacteria were harvested by centrifugation at 5000 rpm for 10 min at 4 °C, resuspended in 50 mM Tris-HCl, 50 mM NaCl, 10 mM EDTA, 0.03% Triton-X-100, pH 7.5, and sonicated. Insoluble material was removed by centrifugation at 14 000 rpm for 40 min at 4 °C. Supernatants containing the $(A\alpha_2$-L1M/L38M$)_2$ four-α-helix bundle and residual bacterial proteins were pooled and heated at 70 °C for 30 min, to denature native proteins, which were then removed by centrifugation at 14 000 rpm for 40 min at 4 °C. The remaining supernatant was loaded onto a C_{18} reversed-phase preparative HPLC column (Vydac, Hesperia, CA), and separated using an aqueous-acetonitrile gradient (20% (v/v) to 80% (v/v) over 60 min) containing 0.1% (v/v) 2,2,2-trifluoroacetic acid at 10 mL/min. The $A\alpha_2$-L1M/L38M (final purity > 99%) eluted at 59% acetonitrile using the absorbance at 280 nm. The $A\alpha_2$-L1M/L38M yield was approximately 20 mg per liter of LB medium. Peptide identity was confirmed with laser desorption mass spectrometry (Protein Chemistry Laboratory, University of Pennsylvania, Philadelphia, PA). The expected molecular weight was 6863.1 Da, and the experimental value was 6869.8 Da.

Circular Dichroism Spectroscopy. Spectra were recorded on a model 62 DS spectropolarimeter (Aviv, Lakewood, NJ), using 2 mm (far-UV region) or 10 mm (near-UV region) path length quartz cells. The cell holder was temperature controlled at 25.0 ± 0.1 °C. The buffer was 10 mM potassium phosphate at pH 7.0. The bandwidth was 1.00 nm, with a scan step of 0.5 nm and an average scan time of 3.0 s.

Denaturation Study. Denaturation of the four-α-helix bundle $(A\alpha_2$-L1M/L38M$)_2$ was followed using circular dichroism spectroscopy, monitoring the ellipticity at 222 nm (Θ_{222}), as described.[15] The measured Θ_{222} as a function of the added denaturant concentration was fit to the equation of Mok et al.[16] describing the unfolding of a dimer (four-α-helix bundle) into two monomers, using a nonlinear least squares routine,

$$\text{fraction folded} = 1 - [[\exp(\Delta G^{H_2O} + m[\text{denaturant}])]/RT]/ [4P(1 + (8P/(\exp(\Delta G^{H_2O} + m[\text{denaturant}])/RT)) - 1)^{1/2}] \quad (1)$$

where ΔG^{H_2O} is the conformational stability of the protein, m is the slope of the unfolding transition, [denaturant] is the molar concentration of GndCl, R is the gas constant, T is the absolute temperature, and P is the molar monomer concentration of $A\alpha_2$-L1M/L38M.

Steady-State Fluorescence Measurements. Binding of halothane to the four-α-helix bundle $(A\alpha_2$-L1M/L38M$)_2$ was determined using steady-state intrinsic tryptophan fluorescence measurements[13] on a RF-5301PC spectrofluorometer (Shimadzu, Columbia, MD). Tryptophan was excited at 280 nm (bandwidth 1.5 nm), and emission spectra (bandwidth 5 nm) were recorded with peaks at 325 nm. The quartz cell had a path length of 10 mm and a Teflon stopper. The temperature of the cell holder was controlled at 25.0 ± 0.1 °C. The buffer was 130 mM NaCl, 20 mM sodium phosphate, pH 7.0. Protein concentration was determined with a UV/vis spectrometer Lambda 25 (Perkin-Elmer, Norwalk, CT), taking ϵ_{280} for tryptophan = 5700 M^{-1} cm^{-1}.[17] Halothane equilibrated bundle protein, in gastight Hamilton (Reno, NV) syringes, was diluted with predetermined volumes of plain protein (not exposed to anesthetic, but

otherwise treated in the same manner) to achieve the final anesthetic concentrations indicated in the figures.

As described previously,[13,18] the quenched fluorescence (Q) is a function of the maximum possible quenching (Q_{max}) at an infinite anesthetic concentration ([anesthetic]) and the affinity of the anesthetic for its binding site (K_d) in the vicinity of the tryptophan residues. From mass law considerations, it then follows that

$$Q = (Q_{max} \cdot [\text{anesthetic}])/(K_d + [\text{anesthetic}]) \qquad (2)$$

Nuclear Magnetic Resonance Measurements. One-dimensional nuclear magnetic resonance spectra were recorded on a Varian Inova 500 MHz instrument with a 90° pulse-acquisition sequence[19] (spectral width of 10 kHz, water presaturated for 1.5 s, 128 scans). The $A\alpha_2$-L1M/L38M concentration was 590 μM in 20 mM phosphate buffer (containing 10% D_2O), pH 7.0. Halothane (40 μL, final concentration 510 μM) was added from a stock solution of 10.0 mM to the NMR tube containing $(A\alpha_2\text{-L1M/L38M})_2$ to yield approximately a 1:1 concentration, resulting in a final $A\alpha_2$-L1M/L38M concentration of 560 μM. The spectra were processed using Felix 2.3 from MSI (San Diego, CA) on a Silicon Graphics (Mountain View, CA) workstation. The spectra were referenced with respect to the water peak (4.81 ppm at 20 °C).

Curve Fitting and Statistics. Unless otherwise noted, best-fit curves were generated with the KaleidaGraph (Version 3.6, Synergy Software, Maywood, NJ, 2003) program. Data are expressed as means ± SD.

Results

I. α-Helical Content and Conformational Stability of the Four-α-Helix Bundle $(A\alpha_2\text{-L1M/L38M})_2$. Circular dichroism spectroscopy was used to measure the α-helical content of the four-α-helix bundle $(A\alpha_2\text{-L1M/L38M})_2$. Figure 4 shows that the $-[\Theta]_{222}$ (in deg cm^2 dmol^{-1}) of $(A\alpha_2\text{-L1M/L38M})_2$ is 21 200. For comparison, the $-[\Theta]_{222}$ of the chemically synthesized $(A\alpha_2\text{-L38M})_2$ four-α-helix bundle is 22 600 deg cm^2 dmol^{-1}.[4] The measured $-[\Theta]_{222}$ for $(A\alpha_2\text{-L1M/L38M})_2$ translates into a percent α-helical content of 66.3% using a value of 32 000 deg cm^2 dmol^{-1} for 100% α-helix.[20]

The conformational stability of the four-α-helix bundle $(A\alpha_2\text{-L1M/L38M})_2$ was determined using chemical denaturation with guanidinium chloride (GndCl). The ellipticity at 222 nm for the four-α-helix bundle was measured as a function of added denaturant, and the data were fit using eq 1. Figure 5 shows that $(A\alpha_2\text{-L1M/L38M})_2$ undergoes full denaturation in the presence of GndCl. The calculated ΔG^{H_2O} and m values for the four-α-helix bundle are -12.2 ± 0.4 kcal/mol and 2.6 ± 0.2 kcal/mol M, respectively. These values compare favorably with the ΔG^{H_2O} and m values of -13.1 ± 0.2 kcal/mol and 2.6 ± 0.1 kcal/mol M obtained with the chemically synthesized $(A\alpha_2\text{-L38M})_2$ four-α-helix bundle.[4]

II. Binding of the Volatile General Anesthetic Halothane to the Hydrophobic Core of the Four-α-Helix Bundle $(A\alpha_2\text{-L1M/L38M})_2$. The binding of halothane to the four-α-helix-bundle $(A\alpha_2\text{-L1M/L38M})_2$ hydrophobic core was followed by tryptophan fluorescence quenching[13,15,21] as shown in Figure 6. Halothane causes a concentration-dependent quenching of the intrinsic W15 fluorescence, without changing the emission maximum, indicating that halothane binds in the vicinity of the indole rings without altering the local dielectric environment. Figure 7a shows a plot of the bundle tryptophan fluorescence as a function of the halothane concentration. Fitting the data using eq 2 yields a $K_d = 120 \pm 20$ μM with a $Q_{max} = 0.96 \pm 0.05$, indicating that the fluorescence of both of the tryptophan residues in the bundle core is quenched by bound anesthetic.

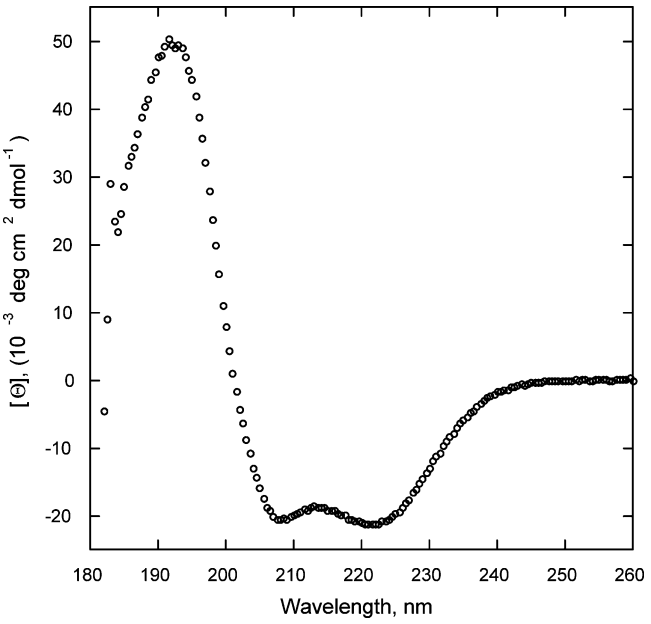

Figure 4. Far-UV circular dichroism spectrum of the four-α-helix bundle $(A\alpha_2\text{-L1M/L38M})_2$ at 3.5 μM in 10 mM potassium phosphate buffer, pH 7.0.

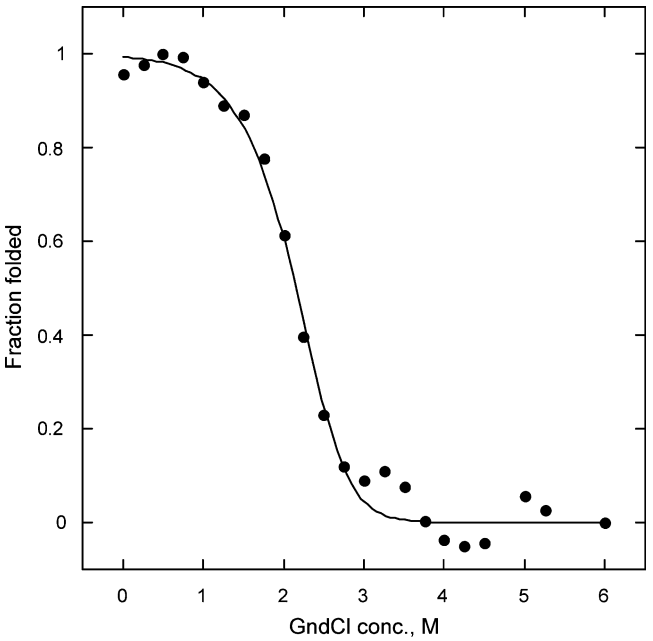

Figure 5. Four-α-helix bundle denaturation curve as monitored by spectropolarimetry at 222 nm. The four-α-helix bundle $(A\alpha_2\text{-L1M/L38M})_2$ concentration was 3.5 μM. The calculated ΔG^{H_2O} and m values are -12.2 ± 0.4 kcal/mol and 2.6 ± 0.2 kcal/mol M, respectively.

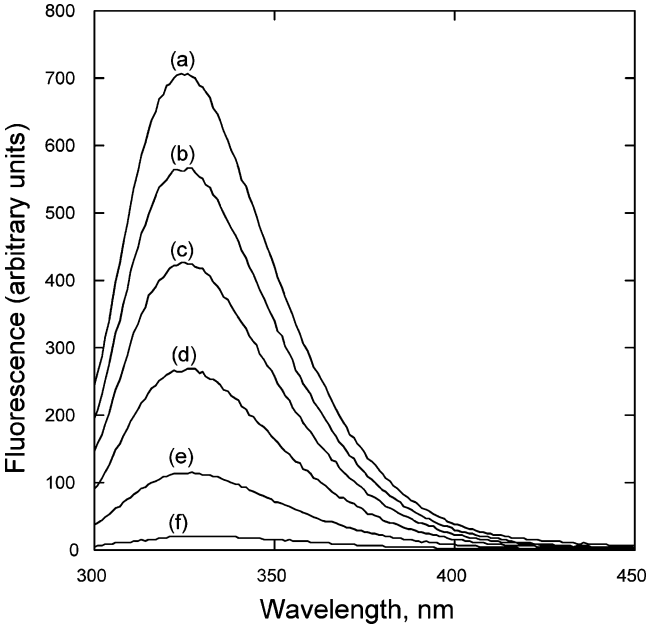

Figure 6. Quenching of the $(A\alpha_2\text{-L1M/L38M})_2$ bundle (1.9 μM) W15 fluorescence by halothane. Excitation was at 280 nm, with the emission maximum at 325 nm. The concentrations of halothane were (a) 0, (b) 50 μM, (c) 100 μM, (d) 250 μM, (e) 1 mM, and (f) 10 mM.

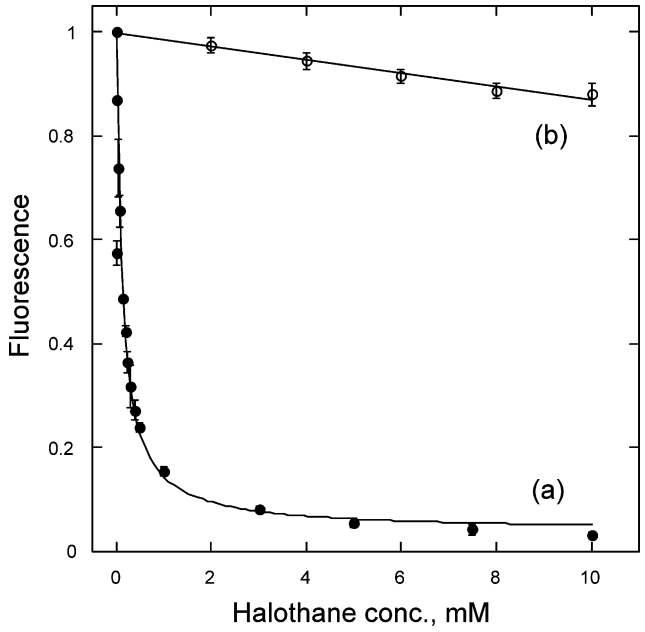

Figure 7. (a) Fluorescence quenching profile for the four-α-helix bundle $(A\alpha_2\text{-L1M/L38M})_2$ by added halothane. Bundle protein concentration was 1.9 μM. Data points are the means of three experiments on separate samples with error bars representing the SD. The line through the data points has the form of eq 2. (b) Effect of halothane on $A\alpha_2$-L1M/L38M (3.8 μM) W15 fluorescence in the presence of 50% (6.9 M) TFE.

The importance of bundle tertiary structural interactions for anesthetic binding is shown in Figure 7b, which demonstrates the diminished quenching of W15 fluorescence in the di-α-helical $A\alpha_2$-L1M/L38M by halothane following bundle dissociation with 2,2,2-trifluoroethanol (TFE). Trifluoroethanol negates the hydrophobic interactions that underlie four-α-helix bundle formation,[22] while maintaining secondary structure.[23] The magnitude of fluorescence quenching in 50% TFE is comparable to that measured when halothane is added to free L-tryptophan in solution,[13,15,21] and

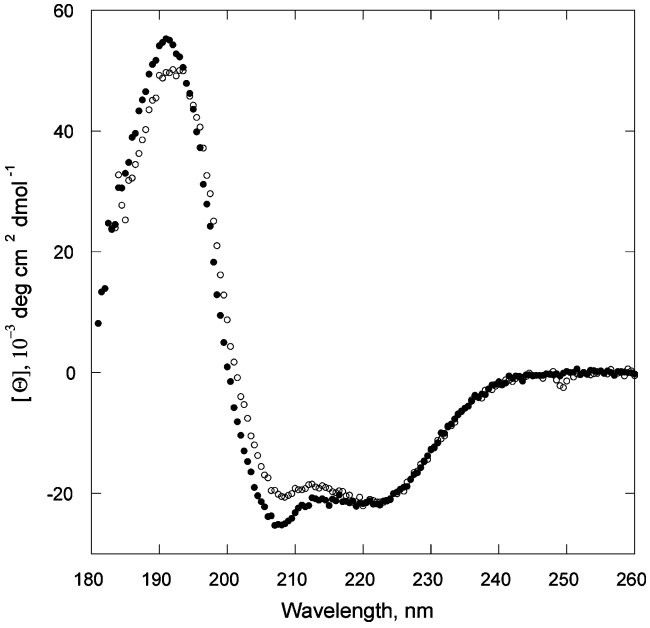

Figure 8. ○, far-UV circular dichroism spectrum of the four-α-helix bundle $(A\alpha_2\text{-L1M/L38M})_2$ at 2.7 μM in 10 mM potassium phosphate buffer, pH 7.0. ●, far-UV circular dichroism spectrum of the di-α-helical peptide $A\alpha_2$-L1M/L38M at 5.4 μM in 10 mM potassium phosphate buffer, pH 7.0, and 50% 2,2,2-trifluoroethanol.

results from collisional encounters between halothane and W15 on the dissociated di-α-helical $A\alpha_2$-L1M/L38M. Figure 8 shows that the secondary structure of the dissociated di-α-helical $A\alpha_2$-L1M/L38M is preserved in 50% TFE. The decrease in the $[\Theta]_{222}/[\Theta]_{208}$ from 1.04 (a value typical for interacting α-helices) in benign buffer to 0.86 (a value characteristic of isolated α-helices) in the presence of 50% TFE supports the interpretation of the results.[20]

III. Near-UV Circular Dichroism Measurements. Figure 9 shows the near-UV CD spectra of $(A\alpha_2\text{-L1M/L38M})_2$ recorded before (a) and after adding an approximately 1:1 concentration (with reference to the presumed concentration of binding sites) of halothane (b). The observed CD signal arises from the two phenylalanines (F12 and F52) and one tryptophan (W15) present per monomer. In the wavelength range 255−270 nm, both phenylalanine and tryptophan absorb; hence the near UV CD in this region reflects the tertiary structure around these residues. Above 270 nm, the near-UV CD represents the tertiary structure around W15 only. In the absence of halothane, the near-UV CD signal for $(A\alpha_2\text{-L1M/L38M})_2$ shows a positive CD with sharp fine structure between 255 and 270 nm. This fine structure is characteristic of phenylalanine residues observed in several structured proteins.[24] Similarly, in the tryptophan range (above 270 nm), the protein shows a negative CD with a strong peak close to 290 nm and fine structure between 290 and 305 nm, which is characteristic of tryptophan residues in structured proteins.[24] The fine structure arises from vibronic transitions in which different vibrational energy levels of the excited state are involved. These near-UV CD patterns indicate that the protein adopts a unique tertiary structure around the aromatic residues. For comparison, unfolded $(A\alpha_2\text{-L1M/L38M})_2$ (in 4 M GndCl, Figure 5) was examined revealing the absence of a near-UV CD signal as shown in Figure 9c.

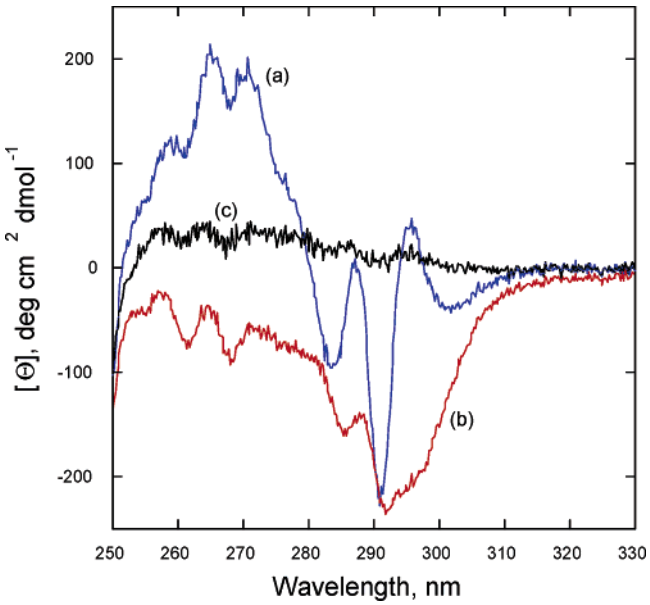

Figure 9. Near-UV circular dichroism spectra of $(A\alpha_2\text{-L1M/L38M})_2$ at 214 μM in 130 mM NaCl, 20 mM sodium phosphate buffer, pH 7.0, and temperature of 25.0 ± 0.1 °C. The (a) blue, (b) red, and (c) black traces represent the spectra before and after adding halothane (430 μM, assuming two binding sites per four-α-helix bundle), and in the unfolded state at 4.0 M GdnCl, respectively.

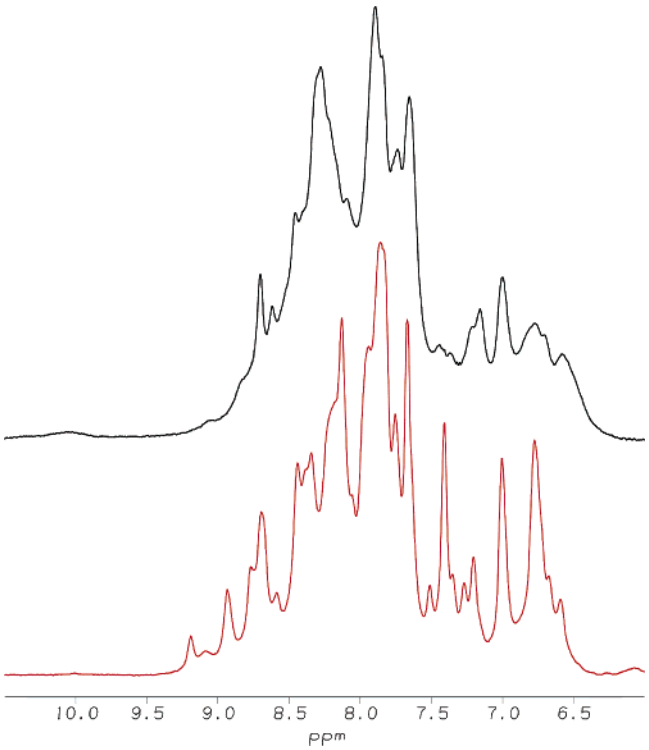

Figure 10. One-dimensional NMR spectra of $(A\alpha_2\text{-L1M/L38M})_2$ (295 μM) in 20 mM phosphate buffer (90% H_2O/10% D_2O), pH 7.0, at a temperature of 20 °C. The black and red lines represent the spectra before and after adding approximately a 1:1 halothane concentration (with reference to the presumed concentration of binding sites). Halothane (510 μM) was added directly to $(A\alpha_2\text{-L1M/L38M})_2$, resulting in a final protein concentration of 280 μM.

With the addition of halothane, clear differences can be seen in the near-UV CD signal, indicating specific binding of halothane to the protein. Although halothane is chiral, it does not absorb in this wavelength range. Below 270 nm, the CD signal changes its sign from positive to negative but retains the same fine structure characteristic of phenylalanine. However, the absolute value decreases as compared to that in the absence of halothane. Because the CD signal in this region comes from four phenylalanine and two tryptophan residues per four-α-helix bundle, the positive and negative signals arising from different aromatic residues may partially cancel each other resulting in a decreased overall intensity, as observed in other structured proteins with multiple aromatic residues.[24] The tryptophan region (above 270 nm) also shows a clear effect of halothane binding on $(A\alpha_2\text{-L1M/L38M})_2$. The protein has the same negative CD intensity; however, the fine structural pattern is different, indicating that in the presence of halothane, the protein adopts a different conformation as compared to that in the absence of halothane. The observed changes in the near-UV CD upon halothane binding also indicate that halothane binds to the protein near the site where the aromatic residues are located. This conclusion is consistent with the observed W15 fluorescence quenching following halothane binding (Figure 6) and also with the location of equivalent binding sites in hydrophobic core layers III and VI (Figure 1C).

IV. Nuclear Magnetic Resonance Study on the Four-α-Helix Bundle $(A\alpha_2\text{-L1M/L38M})_2$. Although a complete structural characterization of the protein and the effect of halothane on its structure will require multidimensional heteronuclear (^{15}N and ^{13}C) experiments, initial exploratory work was performed using proton NMR spectroscopy. Figure 10 shows the one-dimensional (1D) ^1H NMR spectra of $(A\alpha_2\text{-L1M/L38M})_2$ before (top spectrum) and after adding halothane (bottom spectrum). The spectra are shown in the chemical shift range of 10.5−6 ppm. The key resonances to examine in a protein 1D proton spectrum arise from backbone amide protons. In folded, well-structured proteins, the backbone amide protons exhibit a range of chemical shifts due to anisotropic magnetic fields of proximal aromatic and carbonyl groups and resonate between 10.0 and 7.0 ppm.[19] In the case of unstructured, random-coil proteins, these get clustered within a narrow region of 8.5−8.0 ppm. Hence, the chemical shift dispersion of backbone amides is a clear key to determine whether the protein has any stable tertiary structure and with what ease one can determine its three-dimensional structure. Also important are the aromatic ring protons that resonate between 10.5 and 6.0 ppm, predominantly around 7.0 ppm. The aliphatic protons resonate between 6.0 and 1.0 ppm and provide little structural information from 1D NMR spectra of proteins because of significant overlap between aliphatic protons from various residues. In the absence of halothane, the peaks are quite broad and significantly overlapped. This broadness of the resonances may arise from the fact that the protein sequence contains a large degeneracy of amino acid residues (14 glutamates, 12 lysines, 11 leucines, 9 alanines, and 8 glycines, out of 62 amino acids per monomer, Figure 2), and that the four-α-helix bundle exhibits some molten globule character. With the addition of an approximately 1:1 halothane concentration, the peaks become sharper and the chemical shift dispersion increases, indicating that the protein attains a more structured conformation as compared to that in the absence of the anesthetic.

Discussion

Although the in vivo sites of action of the volatile general anesthetics remain to be determined, it is currently argued that membrane proteins in the central nervous system represent likely targets.[8,25] Based upon the few X-ray crystal structures that are available, it is evident that the transmembrane domains of membrane proteins typically consist of bundles of α-helices.[9,26−29] Further, there is evidence that volatile general anesthetics interact directly with the membrane-spanning segments of ligand-gated ion channels and G-protein-coupled receptors.[10−12,30] The ability of an isolated four-α-helix bundle motif to model the transmembrane domains of natural ion channels is therefore being examined to eventually provide detailed structural descriptions of anesthetic−protein interactions, with the long-term objective of understanding the mechanisms of general anesthetic action.

The L1M substitution was not predicted to have a significant effect on the structure and overall thermodynamic stability of $(A\alpha_2\text{-L1M/L38M})_2$ as compared to $(A\alpha_2\text{-L38M})_2$. Methionine is similar to leucine in terms of size (both residues have side-chain volumes of 124 Å^3),[31] helix-forming propensity,[32] and hydrophobicity.[33−35] The $-[\Theta]_{222}$ (in deg cm^2 dmol^{-1}) of $(A\alpha_2\text{-L1M/L38M})_2$ is 21 200, in close agreement with the value of 22 600 for the four-α-helix bundle $(A\alpha_2\text{-L38M})_2$.[4] Removal of the N-termini acetyl groups and the C-terminal carboxyamide groups therefore results in a 6−7% decrease in α-helical content. The conformational stability of the four-α-helix bundle $(A\alpha_2\text{-L1M/L38M})_2$ was -12.1 ± 0.4 kcal/mol, quite comparable to the value of -13.1 ± 0.4 kcal/mol determined for $(A\alpha_2\text{-L38M})_2$.

Halothane binds to the hydrophobic core of $(A\alpha_2\text{-L1M/L38M})_2$ with a $K_d = 120 \pm 20$ μM as determined by the quenching of W15 fluorescence. This represents an approximate 2-fold improvement in the affinity with which the chemically synthesized $(A\alpha_2\text{-L38M})_2$ binds this anesthetic (200 ± 10 μM).[1] This result suggests that there may be sites on in vivo central nervous proteins that also bind halothane with a comparable affinity, which is about one-half of the clinical EC_{50} value of 250 μM.[25] The expressed four-α-helix bundle $(A\alpha_2\text{-L1M/L38M})_2$ differs from $(A\alpha_2\text{-L38M})_2$ in having a methionine residue at position 1 (heptad a position, Figure 1). The effect of the methionine-for-leucine substitution on the affinity of anesthetic binding might be explained by (1) a further optimization of cavity size allowing for improved van der Waals interactions between ligand and protein; (2) a favorable polar contribution from the nucleophilic M1 sulfur atom; or (3) improved access to the cavity (on rate). A further optimization of cavity size might follow from the greater flexibility of the methionine side-chain as compared to leucine.[36−38] Leucine tends to adopt one of two low-energy conformations in an α-helical framework,[39] while the methionine χ^3 torsion angle distributes over the entire range of allowed values.[40] This raises the possibility that the side-chain of M1 may interact directly with the bound anesthetic. The sulfur atom on methionine is more polarizable (1.7-fold) than the corresponding $-CH_2-$ group on leucine.[41] This implies that the dispersion forces that underlie volatile general anesthetic binding to proteins[2] will be enhanced, because their magnitude is proportional to the polarizabilities of the interacting groups. Support for this interpretation is provided by the finding[42] that halothane dissolves 5.2 times better in ethyl methyl sulfide (a model for methionine) than in hexane (a model for leucine).

The circular dichroism signal in the near-UV region (255−320 nm) is caused by the chiral environments of the aromatic side-chains and therefore provides information about the tertiary structure of the protein surrounding these residues. The planar aromatic rings of the phenylalanine and tryptophan residues are not chiral by themselves and hence give rise to no near-UV CD signal.[24] Figure 9 shows that halothane binding results in a change in the structure of the four-α-helix bundle in the vicinity of the aromatic residues W15, F12, and F52. Structural changes in proteins following anesthetic binding have been difficult to detect experimentally[43] but are presumably responsible in many cases for resulting alterations in protein function.

The nuclear magnetic resonance spectroscopy results indicate that halothane binding leads to the appearance of additional peaks in the one-dimensional proton spectrum in the amide region. This is compatible with an anesthetic-induced tightening of the protein structure with an accompanying decrease in dynamics. Using hydrogen exchange,[1] halothane was also shown to stabilize the folded conformation of the four-α-helix bundle $(A\alpha_2\text{-L38M})_2$ by approximately −0.9 kcal/mol. Thus, binding of anesthetic to the four-α-helix bundle scaffolds is associated with a stabilization of the folded conformation of the protein. Halothane has been shown to increase the stability of the native folded conformation of bovine serum albumin using differential scanning calorimetry and hydrogen exchange.[44] Further, both halothane and isoflurane stabilize the native folded state of albumin to thermal denaturation as followed by circular dichroism spectroscopy.[45] In addition to indicating specific binding to the native protein conformer, such stabilization may constitute a fundamental mechanism whereby anesthetics reversibly alter protein function.

Because the four-α-helix bundle $(A\alpha_2\text{-L1M/L38M})_2$ is composed of only 124 residues and is expressed in *E. coli*, the current study opens the way for labeling with the ^{13}C and ^{15}N isotopes to obtain a system with NMR signals of interest.[46] The current results suggest that this four-α-helix bundle represents an attractive system for atomic-level structural studies in the presence of bound anesthetic. Such studies will provide much needed insight into how volatile anesthetics interact with biological macromolecules and will provide guidelines regarding the general architecture of binding sites on native central nervous system proteins.

Acknowledgment. This work was supported by NIH GM55876. Mass spectrometry was performed at the Protein Chemistry Laboratory, University of Pennsylvania, Philadelphia, PA.

References and Notes

(1) Johansson, J. S.; Scharf, D.; Davies, L. A.; Reddy, K. S.; Eckenhoff, R. G. *Biophys. J.* **2000**, *78*, 982.
(2) Eckenhoff, R. G.; Johansson, J. S. *Pharmacol. Rev.* **1997**, *49*, 343.
(3) Manderson, G. A.; Michalsky, S. J.; Johansson, J. S. *Biochemistry* **2003**, *42*, 11203.

(4) Manderson, G. A.; Johansson, J. S. *Biochemistry* **2002**, *41*, 4080.
(5) Johansson, J. S.; Solt, K.; Reddy, K. S. *Photochem. Photobiol.* **2003**, *77*, 89.
(6) Zhang, T.; Johansson, J. S. *Biophys. J.* **2003**, *85*, 3279.
(7) Zhang, T.; Johansson, J. S. *Biophys. Chem.* **2005**, *113*, 169.
(8) Rudolph, U.; Antkowiak, B. *Nat. Rev. Neurosci.* **2004**, *5*, 709.
(9) Miyazawa, A.; Fujiyoshi, Y.; Unwin, N. *Nature* **2003**, *423*, 949.
(10) Eckenhoff, R. G. *Proc. Natl. Acad. Sci. U.S.A.* **1996**, *93*, 2807.
(11) Chiara, D. C.; Dangott, L. J.; Eckenhoff, R. G.; Cohen, J. B. *Biochemistry* **2003**, *42*, 13457.
(12) Ishizawa, Y.; Pidikiti, R.; Liebman, P. A.; Eckenhoff, R. G. *Mol. Pharmacol.* **2002**, *61*, 945.
(13) Johansson, J. S.; Eckenhoff, R. G.; Dutton, P. L. *Anesthesiology* **1995**, *83*, 316.
(14) Stemmer, W. P. C.; Crameri, A.; Ha, K. D.; Brennan, T. M.; Heynecker, H. L. *Gene* **1995**, *164*, 49.
(15) Johansson, J. S.; Gibney, B. R.; Rabanal, F.; Reddy, K. S.; Dutton, P. L. *Biochemistry* **1998**, *37*, 1421.
(16) Mok, Y.-K.; De Prat Gay, G.; Butler, J. P.; Bycroft, M. *Protein Sci.* **1996**, *5*, 310.
(17) Edelhoch, H. *Biochemistry* **1967**, *6*, 1948.
(18) Johansson, J. S. *J. Biol. Chem.* **1997**, *272*, 17961.
(19) Cavanagh, J.; Fairbrother, W. J.; Palmer, A. G.; Skelton, N. J. *Protein NMR Spectroscopy: Principles and Practice*; Academic Press: San Diego, CA, 1996.
(20) Lau, S. Y. M.; Taneja, A. K.; Hodges, R. S. *J. Biol. Chem.* **1984**, *259*, 13253.
(21) Johansson, J. S.; Rabanal, F.; Dutton, P. L. *J. Pharmacol. Exp. Ther.* **1996**, *279*, 56.
(22) Zhou, N. E.; Kay, C. M.; Hodges, R. S. *J. Biol. Chem.* **1992**, *267*, 2664.
(23) Jasanoff, A.; Fersht, A. R. *Biochemistry* **1994**, *33*, 2129.
(24) Kelly, S. M.; Price, N. C. *Curr. Protein Pept. Sci.* **2000**, *1*, 349.
(25) Franks, N. P.; Lieb, W. R. *Nature* **1994**, *367*, 607.
(26) Doyle, D. A.; Morais Cabral, J.; Pfuetzner, R. A.; Kuo, A.; Gulbis, J. M.; Cohen, S. L.; Chait, B. T.; MacKinnon, R. *Science* **1998**, *280*, 69.
(27) Toyoshima, C.; Nakasako, M.; Nomura, H.; Ogawa, H. *Nature* **2000**, *405*, 647.
(28) Bass, R. B.; Strop, P.; Barclay, M.; Rees, D. C. *Science* **2002**, *298*, 1582.
(29) Dutzler, R.; Campbell, E. B.; MacKinnon, R. *Science* **2003**, *300*, 108.
(30) Mascia, M. P.; Trudell, J. R.; Harris, R. A. *Proc. Natl. Acad. Sci. U.S.A.* **2000**, *97*, 9305.
(31) Richards, F. M. *J. Mol. Biol.* **1974**, *82*, 1.
(32) O'Neil, K. T.; DeGrado, W. F. *Science* **1990**, *250*, 646.
(33) Nozaki, Y.; Tanford, C. *J. Biol. Chem.* **1971**, *246*, 2211.
(34) Urry, D. W.; Gowda, D. C.; Parker, T. M.; Luan, C. H.; Reid, M. C.; Harris, C. M.; Pattanaik, A.; Harris, R. D. *Biopolymers* **1992**, *39*, 1243.
(35) Wimbley, W. C.; White, S. H. *Nat. Struct. Biol.* **1996**, *3*, 842.
(36) Bernstein, H. D.; Poritz, M. A.; Strub, K.; Hoben, P. J.; Brenner, S.; Walter, P. *Nature* **1989**, *340*, 482.
(37) O'Neil, K. T.; DeGrado, W. F. *Trends Biochem. Sci.* **1990**, *15*, 59.
(38) Gellman, S. H. *Biochemistry* **1991**, *30*, 6633.
(39) McGregor, M. J.; Islam, S. A.; Sternberg, M. J. *J. Mol. Biol.* **1987**, *198*, 295.
(40) Janin, J.; Wodak, S.; Levitt, M.; Maigret, B. *J. Mol. Biol.* **1978**, *125*, 357.
(41) Fersht, A. R.; Dingwall, C. *Biochemistry* **1979**, *18*, 1245.
(42) Johansson, J. S.; Zou, H. *Biophys. Chem.* **1999**, *79*, 107.
(43) Johansson, J. S.; Eckenhoff, R. G. In *Neural Mechanisms of Anesthesia*; Antognini, J., Carstens, E., Raines, D., Eds.; Humana Press: Totowa, NJ, 2002; pp 395−412.
(44) Eckenhoff, R. G.; Tanner, J. W. *Biophys. J.* **1998**, *75*, 477.
(45) Johansson, J. S.; Zou, H.; Tanner, J. W. *Anesthesiology* **1999**, *90*, 235.
(46) Wüthrich, K. *Acta Crystallogr.* **1995**, *D51*, 249.

BM049226A